SUPPLEMENTARY INFORMATION

Asian Zika virus strains target CD14$^+$ blood monocytes and induce M2-skewed immunosuppression during pregnancy

Suan-Sin Foo[1], Weiqiang Chen[1], Yen Chan[2], James W. Bowman[1], Lin-Chun Chang[1], Younho Choi[1], Ji Seung Yoo[1], Jianning Ge[1], Genhong Cheng[3], Alexandre Bonnin[4], Karin Nielsen-Saines[5], Patrícia Brasil[6], Jae U. Jung[1]*

[1]Department of Molecular Microbiology and Immunology

[2]Division of Maternal-Fetal Medicine, Department of Obstetrics and Gynecology

Keck School of Medicine, University of Southern California, Zilkha Neurogenetic Institute, 1501 San Pablo Street, Los Angeles, CA 90033, USA.

[3]Department of Microbiology, Immunology and Molecular Genetics, University of California, Los Angeles, CA 90095, USA.

[4]Zilkha Neurogenetic Institute and Department of Cell and Neurobiology

Keck School of Medicine, University of Southern California, Zilkha Neurogenetic Institute, 1501 San Pablo Street, Los Angeles, CA 90033, USA.

[5]Division of Pediatric Infectious Diseases, David Geffen School of Medicine, University of California, Los Angeles, Marion Davies Children's Health Center, 10833 LeConte Avenue, Los Angeles, CA 90095, USA.

[6]Laboratório de Pesquisa Clínica em Doenças Febris Agudas, Instituto Nacional de Infectologia Evandro Chagas, FIOCRUZ, 4365 Avenida Brasil, Rio de Janeiro – RJ, 21040-360, Brazil.

*Correspondence

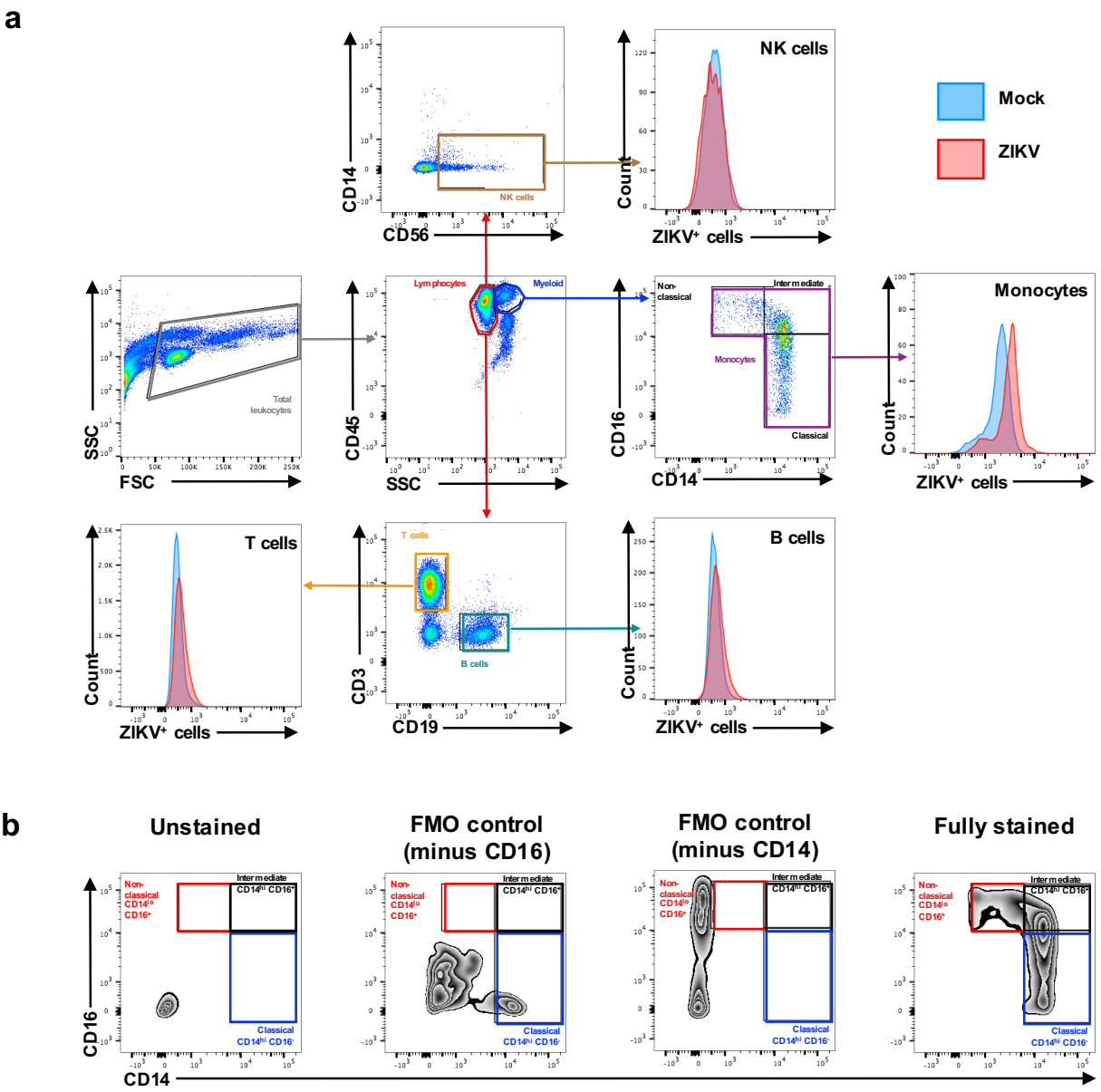

Supplementary Figure 1. Gating strategy for each immune subset within PBMCs. PBMCs were isolated from whole blood of healthy donors for FACS surface staining. **a**, Major blood immune subsets which include $CD3^{+}$ $CD19^{-}$ T cells, $CD3^{-}$ $CD19^{+}$ B cells and $CD14^{-}$ $CD56^{+}$ NK cells were gated from $CD45^{hi}$ SSC^{lo} lymphocyte population, while $CD14^{hi/lo}$ $CD16^{+/-}$ monocytes were gated from $CD45^{hi}$ SSC^{hi} myeloid cells. Gating of $ZIKV^{+}$ cells were based on total population of gated monocytes/NK cells/T cells/B cells. **b**, Specific gating strategy for monocyte subsets with the use of fluorescence minus one (FMO) controls.

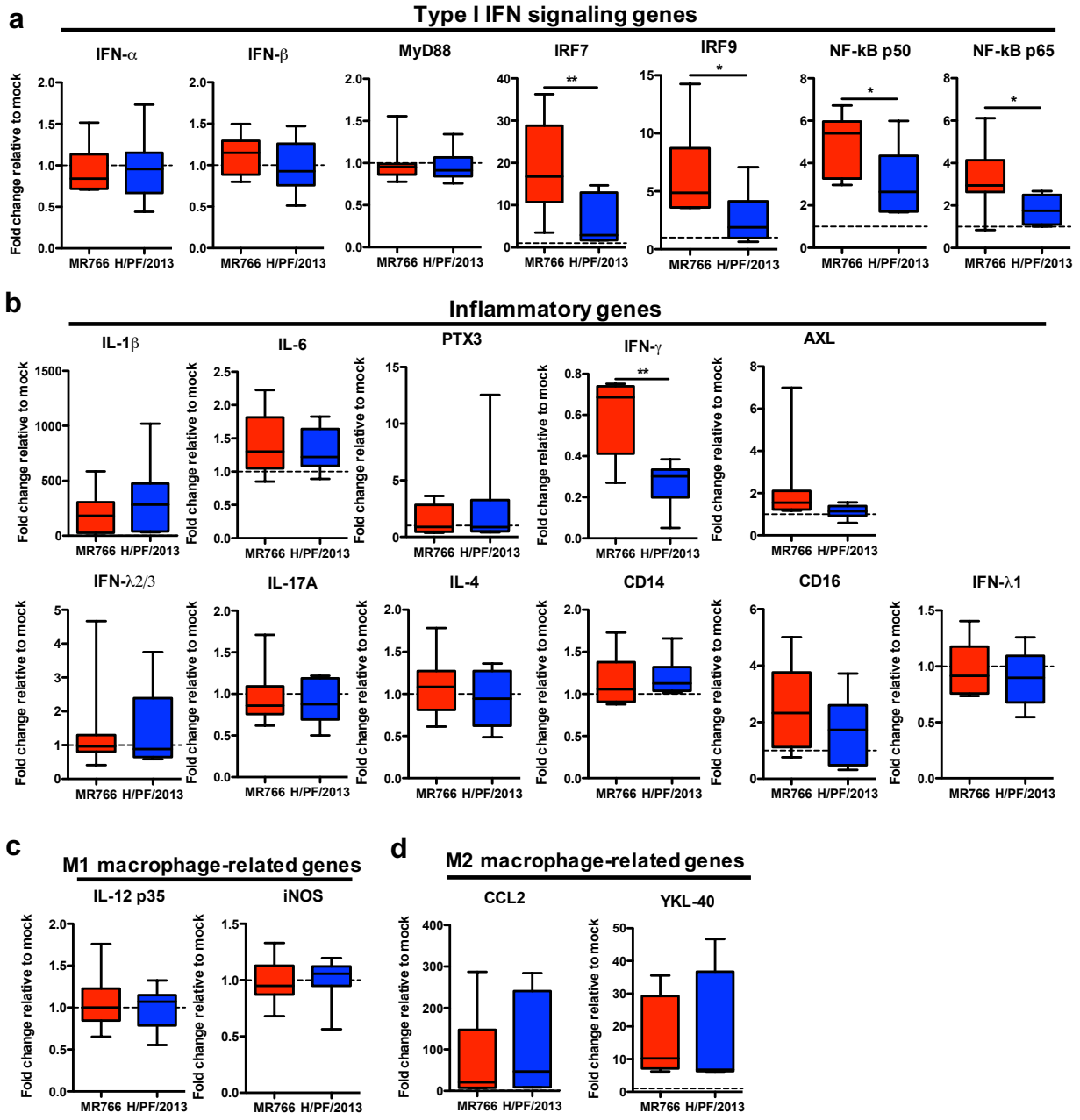

Supplementary Figure 2. Differential gene induction profiles of PBMCs following infection with different ZIKV lineages. Gene expression profiling of PBMCs isolated from mock- or ZIKV-infected (MOI 1) whole blood of healthy donors (n = 8) at 24 hpi. Gene expression of **a**, type I IFN-signaling genes, **b**, inflammatory genes, **c**, M1 macrophage-related genes and **d**, M2 macrophage-related genes were normalized to GAPDH and expressed as fold change relative to mock controls. Data (mean ± SEM) were presented in box plot showing upper (75%) and lower (25%) quartiles, with horizontal line as median and whiskers as maximum and minimum values observed. * $P < 0.05$, ** $P < 0.01$, Mann-Whitney U test.

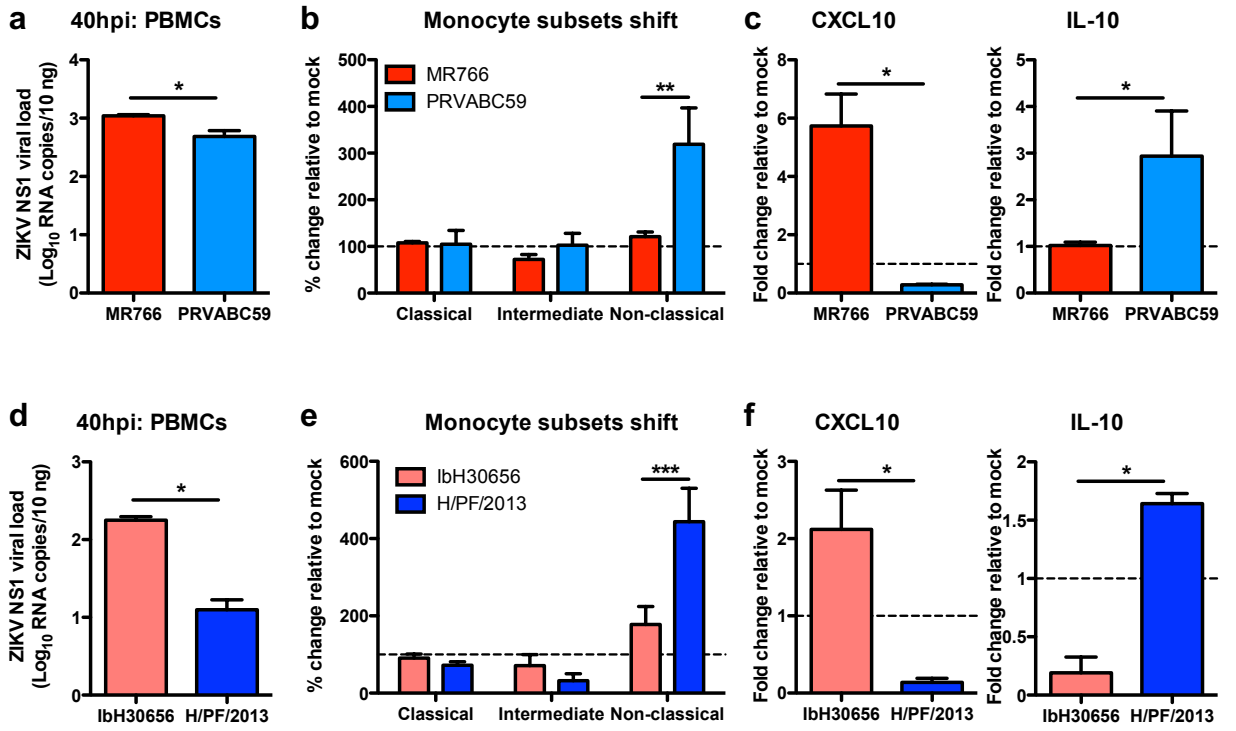

Supplementary Figure 3. Different virological and immunologic traits between African and Asian lineage ZIKV strains. Whole blood from healthy donors (*n* = 3) were infected with different ZIKV strains for 40 h prior to the purification of PBMCs. Infection with MR766 (African ZIKV) and PRVABC59 (Asian ZIKV) was performed at MOI 1, while IbH30656 (African ZIKV) and H/PF/2013 (Asian ZIKV) was performed at MOI 0.1. **a**,**d**, Viral burdens of total PBMCs were detected using viral load qRT-PCR with the specific probes and primers against the ZIKV NS1 RNA. **b**,**e**, FACS analyses were performed to determine classical ($CD14^{+}$ $CD16^{-}$), intermediate ($CD14^{hi}$ $CD16^{+}$) and non-classical ($CD14^{lo}$ $CD16^{+}$) monocyte subsets of mock- and ZIKV-infected PBMCs. **c**,**f**, Expression of *CXCL10* and *IL-10* genes were normalized to *GAPDH* and expressed as fold changes relative to mock controls. Data (mean ± SEM) were presented in box plot showing upper (75%) and lower (25%) quartiles, with horizontal line as median and whiskers as maximum and minimum values observed. * $P < 0.05$, ** $P < 0.01$, Mann-Whitney *U* test in (**a**, **c**, **d**,**f**) or two-way ANOVA, Bonferroni post-test in (**b**,**e**).

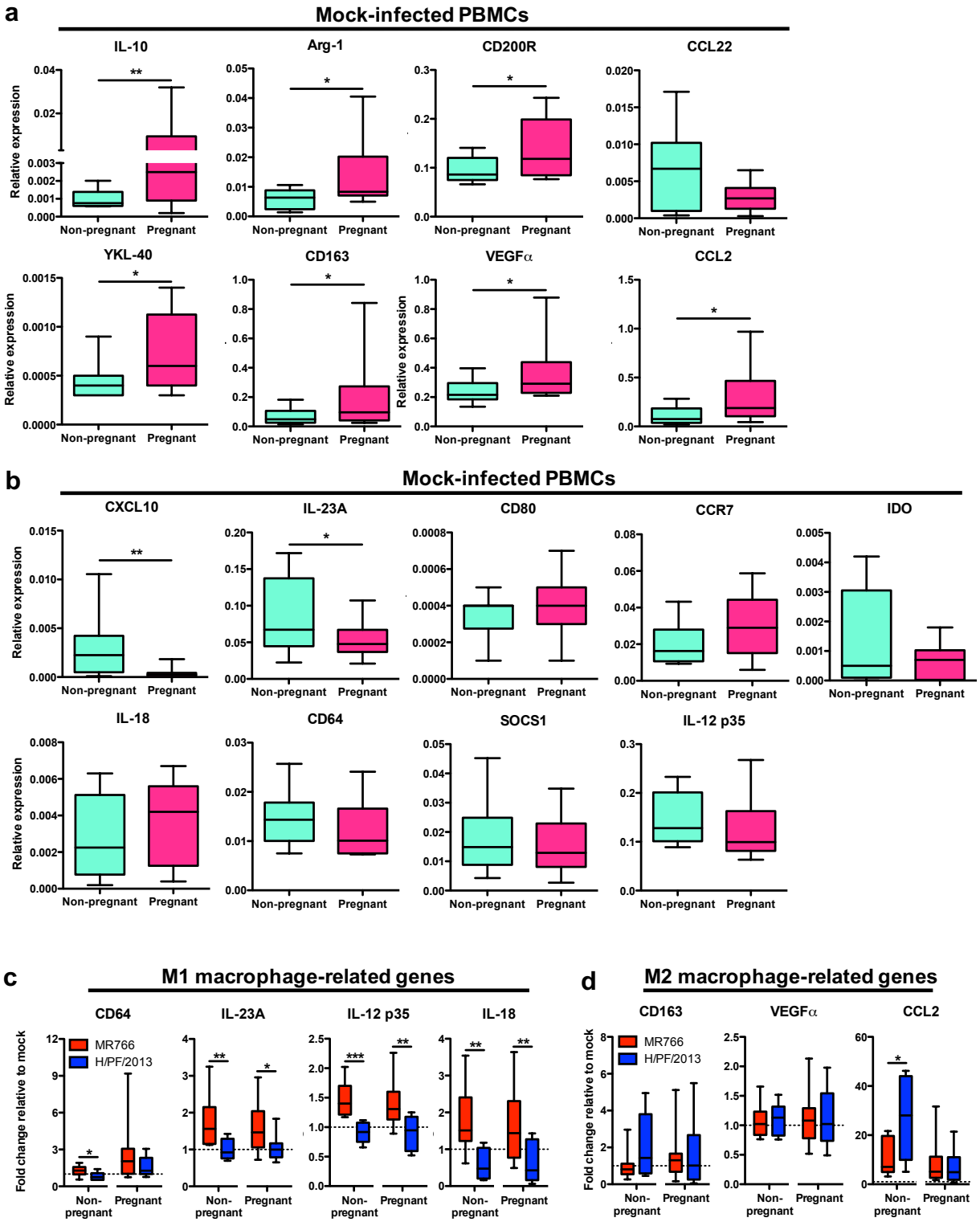

Supplementary Figure 4. Pregnancy primes blood immunity towards M2-skewed immunosuppression, which was further amplified upon Asian ZIKV infection. Gene expression profiling of PBMCs isolated from mock- or ZIKV-infected (MOI 1) whole blood of non-pregnant (n = 10) and pregnant women (n = 5 per trimester) at 40 hpi. Basal expressions of a,

M2 macrophage-related genes, and b, M1 macrophage-related genes, were determined in mock-infected specimens. Gene expressions were normalized to GAPDH and expressed as relative expression. Additional c, M1 macrophage-related genes and d, M2 macrophage-related genes expressions were determined. Gene expressions were normalized to *GAPDH* and expressed as fold change relative to mock controls. Data (mean ± SEM) were presented in box plot showing upper (75%) and lower (25%) quartiles, with horizontal line as median and whiskers as maximum and minimum values observed. * $P < 0.05$, ** $P < 0.01$, Mann-Whitney *U* test.

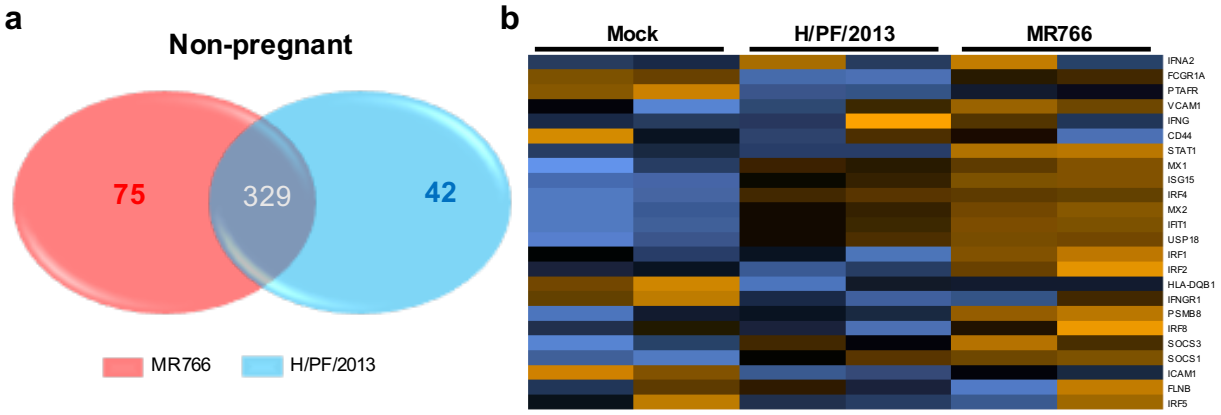

Supplementary Figure 5. Nanostring analysis of non-pregnant women's monocyte specimens. Pan monocytes which include classical ($CD14^{+}$ $CD16^{-}$), intermediate ($CD14^{hi}$ $CD16^{+}$) and non-classical ($CD14^{lo}$ $CD16^{+}$) monocyte subsets were isolated from mock- and ZIKV-infected (MOI 1) PBMCs harvested at 40 hpi. Whole cell lysates of ~10,000 cells/specimen were subjected to NanoString multiplex gene analysis using Human Myeloid panel consisting of ~600 genes. a, Venn diagram representation of the numbers of differentially induced genes between MR766 (African ZIKV) and H/PF/2013 (Asian ZIKV) of non-pregnant women's monocytes specimens. b, Heat map representation of IFN-signaling pathway.